Astron. Astrophys. 322, 646–652 (1997)

ASTRONOMY
AND
ASTROPHYSICS

A solar model with improved subatmospheric stratification

H. Schlattl, A. Weiss, and H.-G. Ludwig

Max-Planck-Institut für Astrophysik, Postfach 1523, D-85740 Garching, Germany

Received 4 November 1996 / Accepted 3 December 1996

Abstract. The calculated intermediate and high degree p-mode frequencies of standard solar models show greater disagreement with the observations than low degree modes. This leads to the conclusion that the subatmospheric structure of the models has to be improved. We are presenting solar models with up-to-date input physics and controlled numerical accuracy of 10^{-5}. For the outer boundary condition we use synthetic atmospheres fitted to the interior solution at $\tau \approx 20$. In addition, a spatially variable mixing length parameter is employed to reproduce the pressure-temperature stratification of the outer convective zone calculated by 2D-hydrodynamical models we used for comparison. With this changed subatmospheric structure we could improve the agreement between predicted and observed p-mode frequencies in our solar models.

Key words: Sun: interior; oscillations

1. Introduction

In the last few years the agreement between observed and theoretical solar p-mode frequencies has been improved considerably (for a review see Christensen-Dalsgaard et al. 1996). Among the residual discrepancies, there is still the fact that the intermediate and high degree frequencies are showing the greatest deviations (Gabriel 1994a). Gabriel (1994b and 1996) has demonstrated that ad-hoc modifications of the opacities in the outer layers along with the introduction of a variable mixing length can lead to a significant improvement of the models. However, up to now no physically motivated solar models have been calculated that aim at an improvement of the subphotospheric layers.

To attack this problem, one recognizes that stellar and many solar model calculations treat the atmospheres still in terms of the Eddington grey approximation or the empirically found Krishna Swamy (1966) T–τ relation (e.g. Bahcall & Pinsonneault 1995 or Guenther et al. 1996) which are very similar for $\tau \gtrsim 0.3$. While this might be sufficient for general purposes, the atmospheric and subphotospheric structure will differ slightly from the real solar structure. At the present level of observational accuracy this difference might already be significant. At the same time, highly sophisticated stellar atmosphere models have become available. This allows to use the bottom of these models for the outer boundary conditions of the interior stellar models. The fitting point need not be the usual $\tau = 2/3$ optical depth – and should not, because only at higher optical depth will the diffusion approximation become excellent. Besides yielding boundary conditions the atmosphere models will also give an improved model for the structure of the outermost solar regions.

Since the atmospheres extend to depths unstable to convection, one gets a *local* description of convection close to the photosphere. The temperature gradient in that region has to pass smoothly into that of the interior model. Quite naturally, one expects that a description employing a single mixing length parameter will prove to be insufficient. Although we still use mixing length theory to model convection, we will introduce a variable mixing length, whose depth dependency is guided by the atmospheric and additional 2D-hydrodynamical models.

We begin this paper with a short description of the numerical improvements we have made in our code (Sect. 2). Our aim was to control the numerical accuracy of our solar models. In the same section, we also describe the physical aspects. Section 3 contains the results from three of our models, demonstrating the improvement due to the new atmospheres and other updated input physics. Finally, a short summary and discussion follows in Sect. 4.

2. The solar model code

2.1. Numerical improvements

Our program is based on the latest version of the Garching stellar evolution code, which originated from the Kippenhahn-code (Kippenhahn et al. 1967); in this as in most other stellar evolution programs the spatial and temporal parts of the stellar structure equations are decoupled. The original standard grid adjustment scheme in this and many other stellar codes uses the differences in the structure variables to determine the distribution of the grid points. Reiter et al. (1995) have demonstrated that with this method the solution of the linearized spatial structure equa-

Send offprint requests to: H. Schlattl (schlattl@mpa-garching.mpg.de)

tions can only be guaranteed to an accuracy of $\approx 10^{-4}$ with a reasonable number of grid points. A higher precision would lead to a large increase of grid points, because to describe the curvature in any of the structure variables more precisely, a very low value for the maximum difference between neighbouring points is necessary. But this also increases the number of grid points in almost linear regions and might eventually even lead to numerical problems. Wagenhuber & Weiss (1994) have developed an improved scheme, which is implemented in the program used for the present work. Here, the number and distribution of the grid points of the converged model are checked by a second-order integrator scheme. This method inserts grid points in regions where the gradient of any of the structure variables (radius r, pressure P, temperature T, luminosity L_r) varies and removes points where the run in r, P, T and L_r with mass coordinate (M_r) is nearly linear. It also guarantees that the number and distribution of grid points is adjusted to the desired precision in the solution of the partial differential equations. An accuracy of up to $5\,10^{-6}$ can, for example, be reached with about 3500 grid points, with which it still is possible to calculate a solar model within reasonable computation time.

A possibility to test the accuracy of the numerical solution of the stellar structure equations, proposed by Reiter et al. (1995), is to check the virial theorem and energy conservation. For the traditional grid scheme a level of 10^{-4} can be reached at most (Reiter et al. 1995). With our grid-control method both physical laws are fulfilled with an accuracy better than 10^{-6}, if for the maximal deviation of the linearized from the true curvature a value of $5\,10^{-6}$ is used. As the relative accuracy in the observations of the best determined p-mode frequencies is about 10^{-5}, the numerical precision of our solar models has reached the desired level; this allows to conclude that any remaining difference between model and the Sun is of physical nature, indeed.

The temporal part of the stellar structure equations, comprising the chemical evolution due to nuclear burning and mixing processes, is solved explicitly. To follow the composition changes over a given evolutionary time-step between two subsequent models, this time-step is divided into smaller "chemical" steps (typically about 50), where the elements are alternately burned in a nuclear network and mixed by a diffusion scheme. This subdivision into smaller "chemical" time-steps is a consequence of the fact that in the nuclear network the reaction equations are linearized and solved by an implicit, forward differencing scheme. The abundances of all isotopes participating in the pp- and CNO-cycle are followed explicitly. Within the chemical time-steps temperature and density and thus the reaction rates and diffusion constants are fixed but are not the same for all chemical steps within the full time-step. The change of these values over the evolutionary step is determined by a predictor-corrector procedure. The required agreement between predicted and corrected values of temperature and density at all grid-points typically is 10^{-5} and the resulting number of time-steps for our most accurate solar models is about 2000. By "corrected" we mean the converged values of the next model. If T and ρ had been assumed constant over the whole evolutionary time-step (the traditional method) about 10,000 time-steps would have been necessary for a comparable accuracy.

We add that the general approach to the numerical accuracy of stellar and even solar models is to assume that with an increasing number of grid points and time-steps the accuracy will improve. While this may be true on average, locally the model accuracy might not follow the general precision. Furthermore, a quantitative measure for the accuracy at given resolution is not possible. With our methods these defects have been overcome. (For examples of the influence of numerical accuracy on solar models, see Schlattl 1996.) The systematic errors introduced by the numerical solution of nuclear network and diffusion equation may increase with the number of time-steps and thus limit the accuracy of the temporal part of the stellar structure equations. We have tested the conservation of mass in the diffusion and nuclear network algorithms and find that numerical errors remain below 10^{-7}.

2.2. Standard input physics

We are using up-to-date input physics from several sources for our solar models. For the thermodynamical quantities including the calculation of the gravothermal energy release (cf. Reiter et al. 1995) the MHD- (Hummer & Mihalas 1988, Mihalas et al. 1988, Däppen et al. 1988) or the OPAL-equation of state (Rogers et al. 1996) is used. The opacities used are either those of Rogers & Iglesias (1992) plus Weiss et al. (1990) or Iglesias & Rogers (1996) completed by Alexander & Fergusson (1994)-tables in the low temperature regime. The merging of the latter two sets is done between 6,000 and 10,000 K. The transition is very smooth. The heavy element abundances for the same table sets agree with the Grevesse & Noels (1993) ones. Our homogeneous starting model is a fully convective pre-main sequence model at $L \approx 1.6\,L_\odot$. Some sequences were also started from homogeneous zero-age main-sequence (ZAMS) models. The nuclear reaction rates are taken from Castellani et al. (1996). We take into account the microscopic diffusion of hydrogen, helium, the isotopes of the CNO-cycle and some heavy elements (Ne, Mg, Si). The diffusion constants for pressure, temperature and concentration diffusion in the radiative zone are determined from the routine of Thoul et al. (1994). The diffusion equation is solved for the entire Sun, where in the convective zone an effective diffusion constant from the convective velocity of the mixing length theory is calculated, which leads to instantaneous mixing.

The change in Z arising from diffusion is taken into account in the opacity tables and the OPAL-EOS by interpolating between tables of different Z. As diffusion does not alter the distribution of the different heavy elements more than 3% the error introduced by using the opacities for the Grevesse & Noels (1993) heavy element distribution is negligible.

2.3. Atmosphere

The central improvement of our models as compared to those of other groups concerns the treatment of the atmosphere and

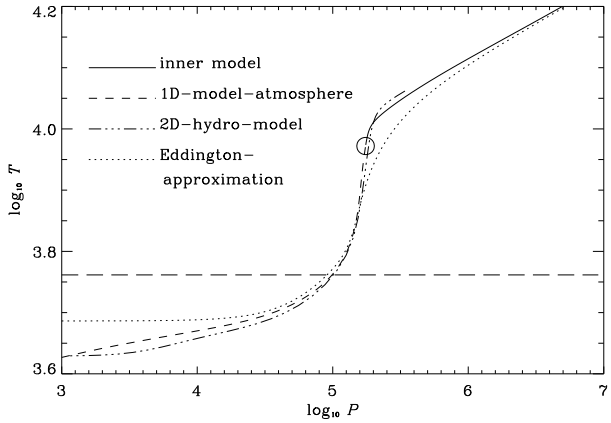

Fig. 1. Temperature-pressure-stratification of our best solar model (solid line) together with that of the model atmosphere used (dashed) in comparison with the 2D-hydrodynamical model (dash-dotted) and a standard solar model with Eddington grey atmosphere and constant α (dotted). The fitting point between interior model and atmosphere is indicated by an open circle; the effective temperature of the Sun is at the long-dashed horizontal line

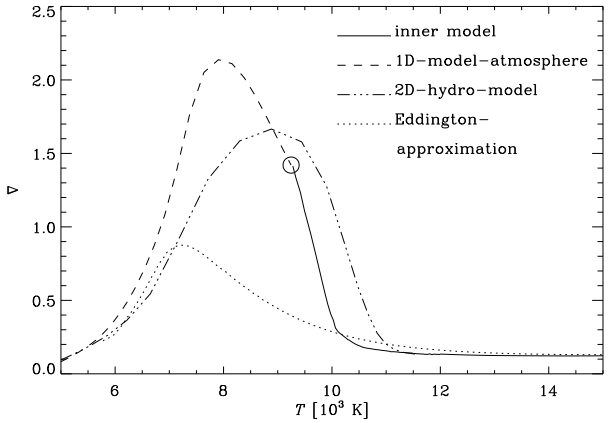

Fig. 2. Temperature gradient $\nabla = \frac{d\ln T}{d\ln P}$ of the models shown in Fig. 1. Only the superadiabatic temperature range is shown.

subphotospheric layers. Whereas the common approach is to use Eddington grey atmosphere down to an optical depth of $\tau = 2/3$ as in our original code, we now apply model atmospheres (Bernkopf 1995, private communication; for a detailed description, see Axer et al. 1994, 1995). These atmospheres are used both for the determination of the outer boundary condition at an optical depth of $\tau \approx 20$ and for the subatmospheric structure. Since they were calculated to fit the theoretical line spectrum of the Sun and because they extend to high optical depth it is necessary to model the outer convective zone in the atmosphere, where the mixing length theory was used. The value for the atmospheric mixing length parameter $\alpha_{\rm at}$ is determined by matching the observed Balmer lines with the ones of the model atmosphere. This leads to a value of 0.5 for $\alpha_{\rm at}$. The temperature gradient between the photosphere and $\tau \approx 20$ is steeper than in model atmospheres of Kurucz (1979), who uses a mixing length parameter of 2.0. We had available a grid of model atmospheres for different effective temperatures and gravities appropriate for the whole main-sequence evolution of the Sun. As they are matched at $\tau \approx 20$ with the inner solar model, the usual diffusion approximation for the radiative energy transport is used only at optical depths greater than 20. This further increases the physical accuracy of the models.

We want to add that the atmosphere tables do not contain thermodynamic quantities, especially the adiabatic gradient Γ_1 which is needed for the calculation of the p-mode frequencies. We used the OPAL-equation of state which is very similar in these temperature- and pressure-ranges to the one used in the calculation of the atmosphere models (Bernkopf 1996, private communication).

The solar model atmosphere has been compared with a 2D-hydrodynamical model for the superadiabatic layers of the present Sun (Freytag et al. 1996); this calculation extends deeper into the Sun. In the 2D-model the radiative energy transport has not been calculated as sophisticated as in the model atmospheres, but convection has been treated hydrodynamically. A comparison between the temperature-pressure stratification of the 1D-atmosphere and the 2D-hydro-envelope (Fig. 1) shows small differences only for $T < T_{\rm eff}$. We add that the run of temperature of the 2D-model (dash-dotted line) as plotted results from averaging over surfaces of same optical depth. The steep temperature gradient at $\log_{10} P \approx 5.2$ of the model atmosphere which mainly results from the low value of $\alpha = 0.5$ agrees very well with the 2D-model; a solar model with the usual Eddington grey atmosphere and constant α (obtained from calibrating to the solar radius) fails to reproduce this (dotted line).

Although the two models are in close agreement it should be mentioned that the temperature gradients (∇) show differences (Fig. 2). The 2D-hydro-envelope is, in comparison with the 1D-model atmosphere, less superadiabatic below 9,000 K, but more superadiabatic above it. As the p-mode frequencies are very sensitive to the shape as well as the maximum value of ∇ (Gabriel 1995) this could lead to changes of up to 10 μHz once the 2D-hydrodynamical models instead of the model atmospheres will be combined with the interior models.

Nevertheless, although atmosphere and 2D-hydrodynamical model were calculated with different intentions and methods, they agree rather well and we infer that their description of the subatmospheric structure is close to the real one.

The value of $\alpha_{\rm at} = 0.5$ leads to a discontinuity in the temperature gradient at the outer boundary condition, if a constant mixing length parameter for the inner model was used. This is the usual approach, where α is determined by the requirement that the solar radius is reproduced (e.g. for an Eddington atmosphere we obtain $\alpha \approx 1.7$). To avoid the discontinuity we introduced a spatially varying mixing length parameter. The (arbitrary) transition function was chosen to model the temperature-pressure stratification of the 2D-model as it extends deeper into the Sun

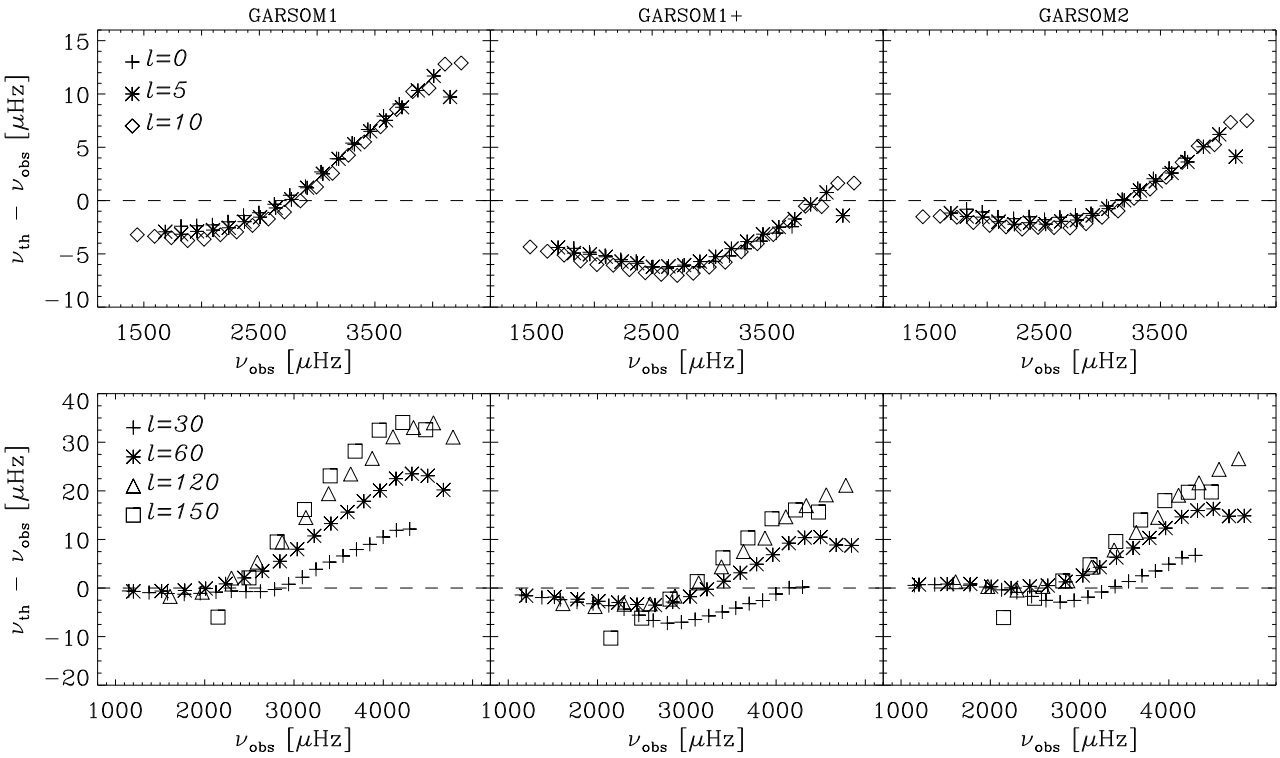

Fig. 3. Difference between observed p-mode frequencies and those predicted by GARSOM1, GARSOM1+, and GARSOM2, resp. Observational values are from Libbrecht et al. (1990) and Elsworth et al. (1994). Upper panels: low l-values; lower panels: intermediate l-values

than the model atmosphere does. With the function

$$\alpha(T) = f(T) \times \alpha_{\rm int} + (1 - f(T)) \times \alpha_{\rm at}$$

where

$$f(T) = \left(1 + \exp\left(\frac{T_0 - T}{\Delta T}\right)\right)^{-1}$$

and the parameters T_0 and ΔT being 10 300 resp. 180 K we obtain a temperature–pressure relation (Fig. 1; solid line) which is very similar to that of the 2D-hydrodynamical model. $\alpha_{\rm int}$ remains a free parameter which has to be fitted to obtain the solar values of effective temperature and luminosity. The $\alpha(T)$-relation as well as the parameters appearing in it have been kept constant for the whole solar evolution.

3. Results

In order to demonstrate the improvements due to the new stratification in the superadiabatic layers, we are comparing two solar models, labeled "GARSOM1" and "GARSOM1+", which both were calculated with the same physical assumptions and data, the sole difference between them being that in GARSOM1 the Eddington approximation for the atmosphere was used, whereas in GARSOM1+ the LTE-atmosphere and subphotosphere models described in Sect. 2 were applied. For the opacities we took OPAL-tables in the version of 1992 (Rogers & Iglesias 1992), complemented with Weiss et al. (1990)-opacities for the low temperature regions; thermodynamic quantities were from the MHD-equation of state (Hummer & Mihalas 1988, Mihalas et al. 1988, Däppen et al. 1988). The initial model was a ZAMS-model. Helium and heavy element diffusion was included; the diffusion constants were calculated according to Thoul et al. (1994). The resulting final photospheric helium fraction is 0.2460, which agrees very well with the value of 0.2461 obtained from a helioseismological model (Basu et al. 1996).

In Fig. 3 the effects of the improved subatmospheric stratification on the p-mode frequencies are shown. Whereas the absolute error for the low and intermediate frequencies increases somewhat with the new atmosphere, it is reduced strongly for the higher frequencies. Applying the error classification of Guenther et al. (1996), we see a reduction of the "slope-error" for both low and intermediate l-values in model GARSOM1+. Similarly, the "thickness error" (i.e. the spread in error at given frequency) in this model is smaller, in particular for the higher degree modes. However, the "offset error" has increased. The reason for these changes is that generally the frequencies in GARSOM1+ are smaller than in GARSOM1, due to the fact that the temperature in most parts of the convective zone is lower when using the new atmospheric structure, although in the superadiabatic layers it is higher (cf. Fig. 4). The lower temperature leads to a lower sound speed, which reduces preferentially the frequencies of the high frequency-modes (Kiefer et al. 1995).

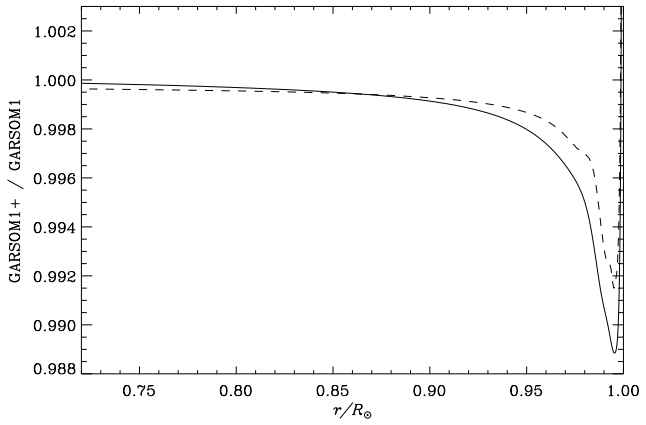

Fig. 4. Temperature (solid line) and sound speed (dashed line) of model GARSOM1+ relative to that of GARSOM1

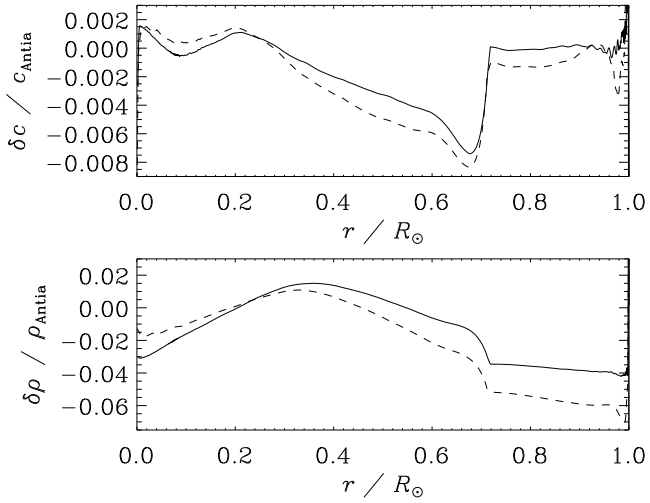

Fig. 5. Difference between our solar models and seismic models of Antia (1996) of sound speed c and density ρ in the sense theoretical – seismic model. The solid line refers to GARSOM2, the dashed line to GARSOM1+.

Our best solar model "GARSOM2" has been calculated with the same physical assumptions as GARSOM1+, but the very latest input-physics data for EOS (OPAL; Rogers et al. 1996) and opacities (Iglesias & Rogers 1996; Alexander & Fergusson 1994). The treatment of diffusion and the modeling of the atmospheric layers is the same as for GARSOM1+. The evolution was started with a pre-main sequence model. The usage of the OPAL95+Alexander- instead of OPAL92+WKM-opacities leads to a shift to higher frequencies for all modes (Fig. 3; right column), i.e. it is reducing the offset-error. The larger shift for the low-degree-modes is an indication for the improvement of the OPAL-opacities in the high temperature-regime. Our best solar model shows an agreement of 5 μHz or better for frequencies between 800 and 2500 μHz with the observations. The slope and thickness errors could again be reduced somewhat but still remain significant. There may be several reasons for this. The neglect of non-adiabatic effects in calculating the frequencies, a bad modeling of convection, or thermal inhomogeneity of the convective zone may alter the frequencies. Zhugzhda & Stix (1994), for example, assume a simple model of alternating up- and down-drafts in the convective zone, which leads to a reduction of the theoretical frequencies with increasing radial order for the radial p-modes (l=0); interestingly, the improvement is of the same order of magnitude as the differences between GARSOM2 and the observations.

The comparison of the run of sound speed and density in GARSOM1+ and GARSOM2 with the seismic model of Antia (1996) (Fig. 5) shows that GARSOM2 differs less down to 0.2 solar radii, whereas GARSOM1+ seems to reproduce the inner 20% of the solar radius better. But there the uncertainties in the seismic model are bigger than the differences between GARSOM1+ and GARSOM2. Thus the OPAL95-opacities together with the OPAL-EOS reproduces the internal structure of the Sun better than the combination of OPAL92-opacities and MHD-EOS. This agrees with results of Guenther et al. (1996). The greatest differences in sound speed and density remain below the convective zone. This may be taken as evidence for a neglected physical process; Richard et al. (1996), for example, find some improvement when postulating additional turbulent mixing just below the convective layer, which counteracts element segregation. We also find that the usage of the OPAL92- instead of the OPAL95-opacities and a higher age of the Sun reduces the discrepancies w.r.t. the seismic model. This may be the reason that the agreement with the seismic model is not as well as in solar models which Gabriel & Carlier (1996) recently have calculated. The center of the Sun seems to be well described by our models, which implies that the neutrino fluxes (see Table 1) are predicted without considerable uncertainty. Therefore the probability of an astrophysical solution of the solar neutrino puzzle could be further reduced.

4. Summary

We have transformed our standard stellar evolution code into an up-to-date solar model code. Particular emphasis has been laid on a controlled numerical accuracy, both in spatial and temporal discretization, since this justifies the conclusion that differences between model and observation indeed have physical reasons. With our new code, we can calculate solar models that are of the same quality as those of other groups. Besides up-to-date input physics data we include helium and metal diffusion, which have become an integral part of the "Standard Solar Model" since Bahcall & Pinsonneault (1992), and pre-main-sequence evolution.

As a further improvement in the calculation of solar models we have abandoned the usual Eddington grey atmosphere fitted to the internal model at $\tau = 2/3$, from where on the diffusion approximation for radiative energy transport is made. Instead, we include boundary conditions from realistic atmospheres, which extend down to an optical depth of 20. The stratification of the atmospheres is also used for the calculation of the p-modes.

Table 1. Selected quantities of our solar models (the solar age is taken as 4.57 Gyr): upper table subscripts refer to the initial composition (i), to surface (S), center (C) and to the bottom of the convective envelope (b.c.); neutrino fluxes (lower table) are given in $s^{-1}cm^{-2}$; the last line gives the predicted flux (in SNU) for the Chlorine and GALLEX experiments.

model	$\alpha_{\rm int}$	Y_i	Z_i	$T_{\rm eff}$ [K]	$\frac{L-L_\odot}{L_\odot}$ [10^{-3}]	$\frac{R_{\rm b.c.}}{R_\odot}$	$T_{\rm b.c.}$ [10^6K]	X_S	Y_S	X_C	Y_C	T_C [10^7K]	ρ_C [$\frac{\rm g}{\rm cm^3}$]
GARSOM1	1.72	0.2732	0.0195	5776	−1.0	0.717	2.15	0.7361	0.2460	0.3378	0.6325	1.56	155
GARSOM1+	3.19	0.2739	0.0195	5776	0.16	0.716	2.13	0.7353	0.2467	0.3370	0.6416	1.57	153
GARSOM2	3.15	0.2707	0.0196	5775	−1.9	0.718	2.14	0.7386	0.2434	0.3436	0.6353	1.57	151

model	$\Phi_{\rm pp}$	$\Phi_{\rm pep}$	$\Phi_{^7{\rm Be}}$	$\Phi_{^8{\rm B}}$	$\Phi_{^{13}{\rm N}}$	$\Phi_{^{15}{\rm O}}$	$\Phi_{^{17}{\rm F}}$	Cl [SNU]	Ga [SNU]
GARSOM1	$5.96\,10^{10}$	$1.41\,10^{8}$	$4.92\,10^{9}$	$5.24\,10^{7}$	$5.69\,10^{8}$	$4.94\,10^{8}$	$5.97\,10^{7}$	7.64	131.4
GARSOM1+	$5.95\,10^{10}$	$1.41\,10^{8}$	$4.98\,10^{9}$	$5.55\,10^{7}$	$5.86\,10^{8}$	$5.11\,10^{8}$	$6.16\,10^{7}$	8.01	132.8
GARSOM2	$5.99\,10^{10}$	$1.41\,10^{8}$	$4.93\,10^{9}$	$5.30\,10^{7}$	$5.78\,10^{8}$	$5.01\,10^{8}$	$6.06\,10^{7}$	7.71	132.1

The value for the mixing-length parameter in the atmospheric model is determined by Balmer-line fits to be 0.5; since a different value for $\alpha_{\rm int}$ is needed for the inner solar model to match the solar radius, it became necessary to introduce a spatially variable $\alpha_{\rm MLT}$. The transition function is chosen in such a way that the deduced superadiabatic envelope stratification resembles that of a 2D-hydrodynamical model, which we used for comparison.

With these changes concerning the outermost parts of our solar models, the resulting p-modes show an improved agreement with the observations, in particular for higher modes and frequencies, i.e. for those oscillations that trace primarily the outer layers of the Sun. The additional usage of the latest opacities and equation of state from the Lawrence Livermore National Laboratory group leads to a relative agreement of $2\,10^{-3}$ or better for all p-modes except for those of highest mode and frequency, where the agreement is $5\,10^{-3}$. Compared to the seismic model of Antia (1996), the sound speed agrees within 10^{-3} except for $0.3 \lesssim r/R_\odot \lesssim 0.7$, where it deviates up to $7\,10^{-3}$. The good agreement of sound speed and density in the central regions of the Sun further rules out an astrophysical solution of the solar neutrino puzzle.

The remaining discrepancies in both p-mode spectrum and sound speed may be reduced by including additional mixing effects just below the convective zone, by further improving the structure in the subatmospheric layers and by taking into account the thermal inhomogeneities in the convective zone in the calculation of the frequencies. This is the line along which further research will be conducted. Finally, from Fig. 1 it is evident that the 2D-hydrodynamical models by Freytag et al. (1996), which in this work were used for comparison only, have the advantage that they extend to regions of the convective envelope, where the temperature gradient has become nearly constant. Since, in addition, they reproduce the optically thin atmospheric layers of the model atmospheres quite well, we will as a next step combine the 2D-hydro-envelopes with the inner model. This will allow to use a constant mixing-length parameter again without losing the improvements we have found in the present paper, although some changes can already be anticipated from Fig. 2. However, the 2D-calculations are resource-intensive and still await completion.

Acknowledgements. We are grateful to Jan Bernkopf for the atmosphere models, to Drs. Alexander and Rogers for providing us on request with customized opacity tables and to Drs. Thoul, Bahcall and Loeb for their diffusion code. Furthermore we would like to thank S. Degl'Innocenti for making us available the p-mode frequencies and Dr. Gabriel, the referee, for very instructive comments. The original stellar evolution program version was that of J. Wagenhuber, whose advice and help we thankfully acknowledge. The work of H. Schlattl and H.-G. Ludwig was supported in part by the "Sonderforschungsbereich SFB-375 Astro-Teilchenphysik" of the Deutsche Forschungsgemeinschaft.

References

Alexander D.R., Fergusson J.W., 1994, ApJ 437, 879
Antia H.M., 1996, A&A 307, 609
Axer M., Fuhrmann K., Gehren T., 1994, A&A 291, 895
Axer M., Fuhrmann K., Gehren T., 1995, A&A 300, 751
Bahcall J.N., Pinsonneault M.H., 1992, Rev. Mod. Phys. 64, 885
Bahcall J.N., Pinsonneault M.H., 1995, Rev. Mod. Phys. 67, 885
Basu S., Christensen-Dalsgaard J., Schou J., Thompson M.J., Tomczyk S., 1996, ApJ 460, 1064
Castellani V. et al., 1994, Phys. Rev. C 50, 4749
Christensen-Dalsgaard J. et al., 1996, Science 272, 1286
Däppen W., Mihalas D., Hummer D.G., Mihalas B., 1988, ApJ 332, 261
Elsworth Y. et al., 1994, ApJ 434, 801
Freytag B., Ludwig H.-G., Steffen M., 1996, A&A 313, 497
Gabriel M., 1994a, A&A 281, 551
Gabriel M., 1994b, A&A 292, 281
Gabriel M., 1995, A&A 302, 271
Gabriel M., 1996, A&A 309, 939
Gabriel M., Carlier F., 1996, A&A (in press)
Grevesse N., Noels A., 1993, Phys. Scripta T47, 133
Guenther D.B., Kim Y.-C., Demarque P., 1996, ApJ 463, 382

Hummer D.G., Mihalas D., 1988, ApJ 331, 794
Iglesias C.A., Rogers F.J., 1996, ApJ 464, 943
Kiefer M., Grabowski U., Stix M., 1995, in: *Stellar Evolution: What Should Be Done*, 32nd Liège Int. Astroph. Coll., 379
Kippenhahn R., Weigert A., Hofmeister E., 1967, *Methods for Calculating Stellar Evolution*, vol. 7 of *Methods in Computational Physics*, 129, New York: Academic Press
Krishna Swamy K.S., 1966, ApJ 145
Kurucz R.L., 1979, ApJS 40, 1
Libbrecht K.G., Woodard M.F., Kaufman J.M., 1990, ApJS 74, 1129
Mihalas D., Däppen W., Hummer D.G., 1988, ApJ 331, 815
Reiter J., Walsh L., Weiss A., 1995, MNRAS 274, 899
Richard O., Vauclair S., Charbonnel C., Dziembowski W.A., 1996, A&A 312, 1000
Rogers F.J., Iglesias C.A., 1992, ApJS 79, 507
Rogers F.J., Swenson F.J., Iglesias C.A., 1996, ApJ 456, 902
Schlattl H., Diploma thesis, Tech. Univ. of Munich, 1996
Thoul A.A., Bahcall J.N., Loeb A., 1994, ApJ 421, 828
Wagenhuber J., Weiss A., 1994, A&A 286, 121
Weiss A., Keady J.J., Magee N.H., 1990, Atomic Data and Nuclear Data Tables 45, 209
Zhugzhda Y., Stix M., 1994, A&A 291, 310

This article was processed by the author using Springer-Verlag LaTeX A&A style file *L-AA* version 3.